Last-Mile Communication Time Requirements of the Smart Grid

Bob Ran
TNO
Delft, The Netherlands
Email: bob.ran@tno.nl

Ebisa Negeri, Nico Baken
Network Architectures and Services
Delft University of Technology
Delft, The Netherlands
Email: e.o.negeri@tudelft.nl, n.h.g.baken@tudelft.nl

Frans Campfens
Alliander Energy Company
The Netherlands
Email: frans.campfens@alliander.com

***Abstract*—With the growing need for sustainable energy, different renewable energy sources as well as low carbon technologies, such as electric vehicles, are increasingly penetrating into the electric power system. The increased deployment of distributed energy sources leads to a decentralized power distribution. The smart grid relies on communication networks to support efficient and decentralized power distribution. To deploy appropriate communication infrastructure for the smart grid, its communication time requirements need to be clearly identified. In this paper, we investigate the last-mile communication time requirements of the smart grid. By closely observing the worst-case node voltage and cable load dynamics in a low-voltage (LV) power grid supporting a neighborhood that is composed of prosumer households, we are able to analyze the worst-case communication time requirements in controlling the LV grid.**

I. Introduction

Currently, there is a growing need for sustainable energy supply. As a result, distributed energy sources (DES), such as photo-voltaic (PV) panels, are increasingly penetrating into the low voltage (LV) power grid. As DES become widely available, the end customers are transforming from passive consumers to active "prosumers" that can locally generate, store and feed their surplus power production back to the grid. With the likely increased domination of prosumers, it is foreseeable that the future smart grid will contain heterogeneous types of prosumers that trade power locally with each other on the grid [1], [2]. Moreover, low carbon technologies, such as electric vehicles (EV) are expected to be widely available. Meanwhile, the intermittence of the DES as well as the large load of the EVs might lead to problems such as peak load, voltage instability, network congestion and difficulty to balance load [3] - [5]. To increase the deployment of DES and EVs and thereby enhance the transition towards sustainable energy, these challenges need to be addressed. Overcoming these challenges requires orchestrating the decentralized power distribution to maintain the stability of the grid, that involves information flows between the parties. Thus, the future smart grid heavily relies on the support of ICT networks [6].

Driven by the dependence of the smart grid on ICT networks, studies related to the ICT infrastructure for the smart grid are capturing the attention of researchers. Various works exist in the literature that address different aspects of ICT network for smart grids that include the architecture of the ICT network [7], reliability of the communication network in the face of failures or attacks [8], scalability of the information processing [9], spectrum utilization of the communication media [10], etc. The references [6] and [11] present overviews of the trends and the requirements of the smart grid communications. One of the major requirements is that the latency of the communication technology should be acceptable for the smart grid services. To determine the acceptable communication latency level, identifying the communication time requirements of the smart grid functions is essential. Identifying the precise communication time requirements of the smart grid helps to choose appropriate telecommunication technologies that have acceptable communication latency. The communication time constraint for the transmission system protection is in the order of a few milliseconds (~10 ms) [12]. In [13], simulative and analytical approaches are used to show that an ICT network based on switched Ethernet in a star topology can guarantee the required time constraint for intra-substation communication. For the LV grid, researchers commonly consider communication networks for demand-response technologies [8], [14], which generally require response times in the order of few seconds to minutes. However, the communication time requirements for node voltage and cable load controls in the LV grid are not identified yet.

In this work, we provide a study about the time requirements for last-mile communication in an LV smart grid. To do so, we consider futuristic neighborhood scenarios with large penetration of DES and EVs, as their increased penetration present enormous challenges to the stability of the LV grid. Under this setting, we closely observe the node voltage and cable load dynamics in the LV grid to determine its worst-case communication time requirements. The rest of this paper is organized as follows. In section II, we present the smart grid functions that could require communication support. Then, we introduce the voltage and load control methods in section III. Afterwards, we present our simulations in section IV, followed by our communication latency computation in section V. Finally, we provide concluding remarks in section VI.

II. The Smart Grid Functions

Communication networks are needed to support smart grid functions, such as load balancing [15], peak shaving [16], local power exchange [1], and voltage and congestion control [18]. Load balancing refers to balancing the power supply and demand, while peak shaving involves reducing the peak power demand. With local power exchange capability, the prosumers can locally trade power with each other and the rest of the grid.

978-3-901882-56-2

Voltage and congestion control involves controlling the power flows in the grid such that the node voltages and the cable loads are maintained within operational limits. The communication time requirements to deploy these functions depend on the frequency of data exchange that they involve. Load balancing and peak shaving involve information exchanges in the order of minutes. For example, the PowerMatcher technology [19] that aims at handling both functions, currently being tested in multiple pilot projects, operates with a communication frequency in the order of minutes. In the literature, communicating price information for local power exchange occurs in time intervals of 15 minutes to an hour [20], [14].

The voltage levels of the nodes in a LV grid network should be within the operational boundaries. In practice, this range is between $90\% - 110\%$ of $230V$[1], i.e. over/undervoltage of only $0.1 \times 230V = 23V$ is tolerated. In addition, each cable has a limited load capacity, and it will be congested if the load it caries exceeds this capacity. The voltage and congestion control are directly linked with the safety of the grid, and they need to monitor the node voltage and cable load dynamics that vary real-time [21], [22]. Hence, they pose more critical requirements on communication time than the other functions of the LV smart grid. Accordingly, we will focus on studying the time requirements of voltage and congestion control as they present the most critical time requirement.

III. Voltage and congestion control in LV grids

In LV grids, fuses are used to disconnect the part of the network that is overloaded/congested, but no active congestion prevention mechanism is in place. On the other hand, there are some techniques that can be used to control voltage levels in LV grids [17]. When a voltage level at the connection point of a PV panel reaches the operational boundary, its inverter curtails or ceases power injection into the grid, thereby reducing the overvoltage. But this voltage control mechanism is not fair because it curtails/ceases the power injection only from the PV panel that has experienced overvoltage at its connection point, although the overvoltage has possibly resulted from the cumulative effect of other energy sources injecting power into the grid. Moreover, the control mechanism is less optimal since more efficient measures, such as increasing the power consumption at another node in the LV grid, could have been taken instead of curtailing the production of the PV panel. The output voltage of some modern transformers can be controlled using automatic transformer tapping technologies, although these transformers are not deployed in LV grids yet.

In the future, when more distributed power sources and devices like EVs penetrate into the LV grid, voltage and congestion control becomes more challenging. Brabandere [18] has pointed out that the future requires more intelligent voltage control mechanisms that coordinate the active/reactive power injected from the energy sources as well as that consumed by devices in the LV grid, such that the voltage levels are kept within the limits. Such control mechanisms can also be used for congestion control. The advantage of this intelligent approach is that fair and optimal decisions can be taken to control under/overvoltages by orchestrating all the resources in the LV grid. These intelligent control mechanisms rely on communication overlay networks to communicate relevant information and control signals. In this work, we investigate the communication time requirements of such foreseeable voltage and congestion control mechanisms of the future.

[1]This is the standard in most of the European countries.

IV. Simulation

A. Simulation setup

We employ a LV grid simulator tool named Gaia [23], which is commonly used by distribution network operators in The Netherlands, to analyze the dynamics of the LV grid. Using Gaia, we undertake load flow analysis that enables us to observe the node voltage levels and the cable load patterns in the network. We have obtained real data on the Dutch LV grid from Alliander[2]. We select the radial LV grid topology as a representative topology, since the Dutch LV grid is mostly radial. In this topology, the houses are connected to a radial string of cable that comes out of the medium voltage to low voltage transformer (MV/LV), as shown in Fig. 1. In the figure, the n_i's represent the connection points where we want to observe the voltage dynamics, and the s_i's represent the segments of the string cable whose load dynamics we want to observe. We adopt the $400V$, $630KVA$ transformer since it is

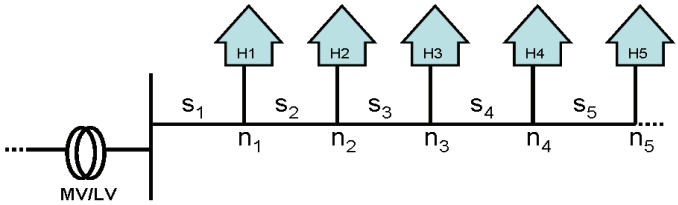

Fig. 1. A typical radial LV grid.

the most commonly used. After analyzing 4000 cables of the radial LV strings with regards to cable type, length and number of connections per string, we found that the largest part of the LV strings have the following properties: (1) 50 mm^2 copper cable or thicker (2) 250 m long or less (3) 27 connections per string or less. While each string cable contains three wires corresponding to the three electrical phases, for our analysis, without lose of generality we consider only the connections on one phase of the string.

In order to observe the critical communication time requirements, we select simulation scenarios that are likely to lead to extreme voltage and load dynamics in the LV grid. For this, we consider the trends in the future neighborhood with regards to both the power production and consumption. From the power production side, different types of distributed power generation types are expected, such as the PV panels, micro-CHPs (combined heat and power plant), fuel cells, wind turbines, etc. The power output of a fuel cell can conveniently be controlled, whereas the power output of a micro-CHP is constant (no variability). The deployment of wind energy is focused on medium- and large-scale wind farms, that are not at a level of neighborhoods (LV grids). At the moment, installing small-scale wind turbines in neighborhoods is not economically attractive. On the other hand, the PV panels are being widely deployed in neighborhoods (connected to

[2]Alliander is a major distribution network operator in The Netherlands that operates approximately 40% of the distribution networks.

LV grids). It is also possible that the PV panels are densely installed in neighborhoods with convenient conditions, such as appropriate roof angle and area. Moreover, the power production of a PV panel could be extremely volatile as it varies with the level of solar radiation, which is not controllable. Thus, the volatility of power production of PV panels is likely to contribute to extreme voltage and load dynamics in the future LV grids, compared to the other energy sources. From the power consumption side, the electric vehicle is a major device leading to extreme voltage and load dynamics in a LV grid due to its excessive power consumption [4], [5] compared to the conventional household appliances. Accordingly, we present two simulation scenarios that are likely to lead to extreme voltage and load dynamics in the LV grid. The first simulation scenario is the case where PV panels are installed at each house. In this scenario, all the houses will simultaneously inject power back to the grid. The second simulation scenario represents the case where each household in the neighborhood possesses electric vehicles, such that the EVs are charged immediately after they come home with the standard charger outlets available at home.

The variation in the production of the PV panels at the households depends on the variation in the solar radiation. The National Renewable Energy Laboratory (NREL) has published [24] a very detailed data set containing 1 Hz solar radiation measurements taken at Oahu, Hawaii over a period of one year. This data set is interesting because its frequency of measurements are quite dense. While the amount of solar radiation in The Netherlands is different from that in Hawaii, the variation of the solar radiation could be comparable as it depends on the speed of the clouds that pass over the sky. Fig. 2 shows the solar radiation pattern of a day that is randomly picked from the data set. As can be observed, the solar radiation has regions that show high volatility, that will result in high variability of the PV productions. We are interested in the high variability regions of the solar radiation because the resulting highly variable PV productions are likely to cause faster variations in the voltage and cable load values in the LV grid, thereby requiring faster response time (critical telecommunication time requirements) before the voltage and cable load boundaries are exceeded.

In order to select the data with the extreme variability, we first subdivided the data sets into intervals of two minutes. Afterwards, the subsets are analyzed to find the intervals with the following properties (x represents radiation level): (1) extreme derivative ($\frac{d(x)}{dt}$), i.e. the steepest rising/falling solar radiation (2) extreme difference between the minimum and maximum radiation ($max(x) - min(x)$) (3) extreme accumulated difference between consecutive radiation values ($\sum_{i=1}^{120} |x(i+1) - x(i)|$).

1) extreme derivative ($\frac{d(x)}{dt}$), i.e. the steepest rising/falling solar radiation.
2) extreme difference between the minimum and maximum radiation ($max(x) - min(x)$).
3) extreme accumulated difference between consecutive radiation values ($\sum_{i=1}^{120} |x(i+1) - x(i)|$).

These properties capture regions of high variability. Eventually, for each of the three variability metrics six intervals with the highest values are selected, giving rise to a total of 18 different data sets. The selected solar radiation intervals are then translated into PV productions, where the capacity of the PV panels at each house is 5kW in total. The power generated from the solar panels corresponding to these extreme time intervals are then used as input to our simulator to observe the resulting voltage and load dynamics in the LV grid.

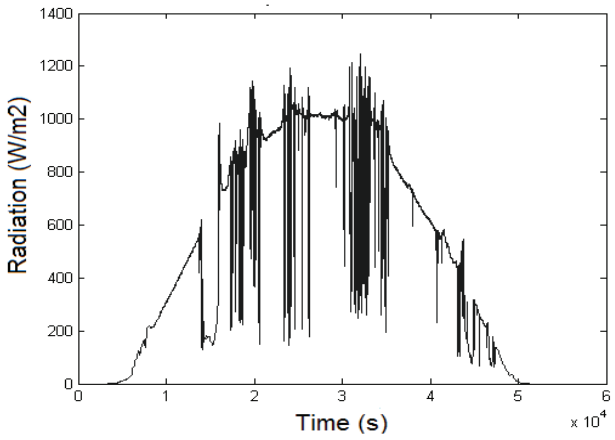

Fig. 2. Solar radiation of a random day form the NREL dataset.

B. Simulation results

First, we present the results of the scenario where PV panels are installed at each household. Plots of the voltage levels at the connection points across the LV string, and the loading of the segments of the radial LV string for a sample 2 minute input data are depicted in Fig. 3 and Fig. 4, respectively. The figures reveal that the operational boundaries are violated at some nodes and string segments in the LV grid. The distribution of the voltage levels and the cable loads can be explained using Ohm's Law and Kirchhoff's Current Law, respectively, as shown in Eq. 1 and Eq. 2, where $M =$ the total number of nodes (string cable segments), $V_0 =$ the voltage level at the transformer, $V_m =$ the voltage at node n_m, $I_m =$ the current flowing through the segment s_m, $R_j =$ the resistance of the segment s_m, and $I_{H_m} =$ the current that is injected from house H_m (see Fig. 1). This explanation is reasonable because LV grids are by nature resistive [17], i.e., $Z = R + jX$, $R >> X$ holds for the segments, where Z is the impedance of a segment, while R and X are the resistive and inductive components of the impedance, respectively.

$$V_m = V_0 + \sum_{j=1}^{M} I_j R_j, m = \{1, 2, ..., M\} \quad (1)$$

$$I_m = I_{m+1} + I_{H_m}, m = \{1, 2, ..., M\} \quad (2)$$

Next, we analyze the simulation results of the voltage and cable load dynamics to extract more useful information. The most important information for our critical time requirement study is how fast the voltage and the load are rising in the worst case. Fig. 5 and Fig. 6 give the corresponding results of the analyses for the voltage and load, respectively. The figures show the time it takes in the worst case to rise to the maximum bound starting from an initial value which is

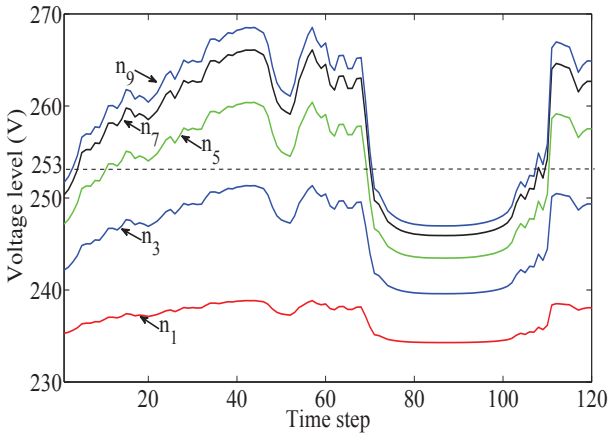

Fig. 3. Voltage level dynamics at different nodes of the LV grid (where n_i represents the i_{th} connection point to the string such that the nodes with larger subscripts are located futher from the transformer).

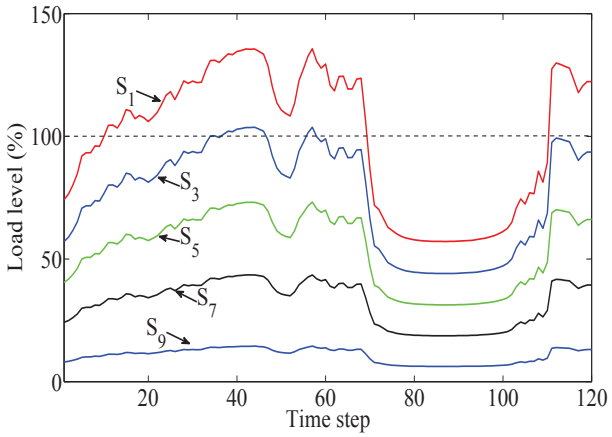

Fig. 4. Load dynamics at different segments of the radial string of the LV grid (where s_i represents the i^{th} segment of the string cable such that the segments with larger subscripts are located further from the transformer).

given as a percentage of the maximum bound. For example, in Fig. 5 we can observe that it takes roughly 0.6 seconds for the voltage to rise from 80% of overvoltage (i.e. 230V + 0.8×23V = 248V) to the maximum possible voltage level (253V). Similarly, we can observe from Fig. 6 that the cable load rises from 80% of the maximum load capacity to the maximum bound in 0.5 seconds.

To see if the slope of the time distributions in Fig. 5 and Fig. 6 depend on the physical properties of the LV grid, we constructed ten different radial LV grid networks with different properties. The difference between the networks is the length of the segments s_i in Fig. 1. The length of the segments s_i used in the ten networks are 5m, 10m, 15m, ..., 50m. Thus, the networks have different values of average electrical resistance between the nodes and the transformer. Our simulation results on these networks reveal that if the average resistance between the nodes and the transformer of the LV grid is larger, the slope of the time distribution in Fig. 5 becomes more steep, while the slope in Fig. 6 becomes less steep. This can be explained as follows. Assuming a resisitive LV network, power

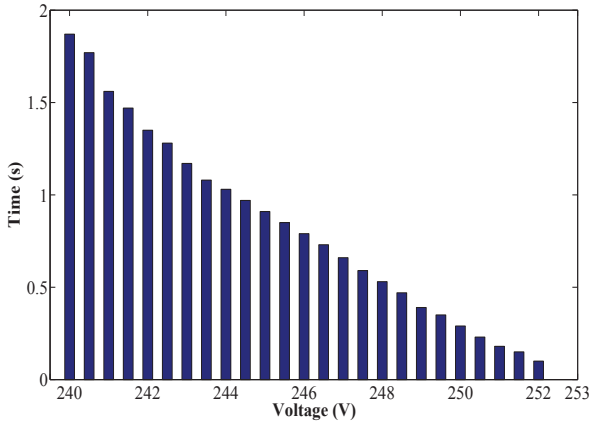

Fig. 5. Time it takes to rise to the maximum voltage in the worst case.

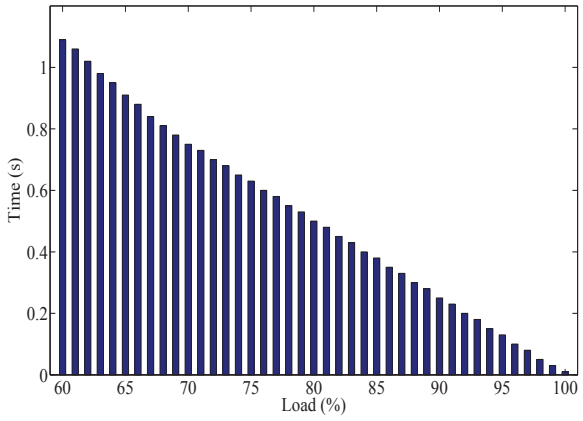

Fig. 6. Time it takes to rise to the maximum load in the worst case.

$P = V \times I$, where $V = R \times I$. Thus, $\Delta I = (\frac{\Delta P}{R})^{1/2}$, and $\Delta V = (\Delta P \times R)^{1/2}$. This means that, for a given rise in the injected power, when the average resistance is larger the voltage rises faster, while the current/load rises slower.

Now, we turn to the second simulation scenario where each house begins to charge its EV as soon as it returns home. Fig. 7 presents the voltage level dynamics at the house connected at the end of the string (n_9) when different number of houses begin to charge their EV exactly at the same time. While the voltage at the end of the string drops slightly when only one EV starts to charge (which occurs at the 2nd second in the figure), large deviation in voltage is observed when more cars start to charge at the same time. A similar property is observed for the load in the segment of the radial string closest to the transformer (s_1), where a larger rise in the load occurred with more EVs charging simultaneously. In reality, chances are very slim that two or more EVs will begin to charge within the same second. Thus, we can assume that EV charging does not cause voltage and load dynamics at a sub-second scale, i.e. whenever the operational boundaries are reached, we have at least one second to control the charging rate of the EVs.

Comparing the results in the two scenarios, the productions of the PVs lead to more time-critical voltage and load

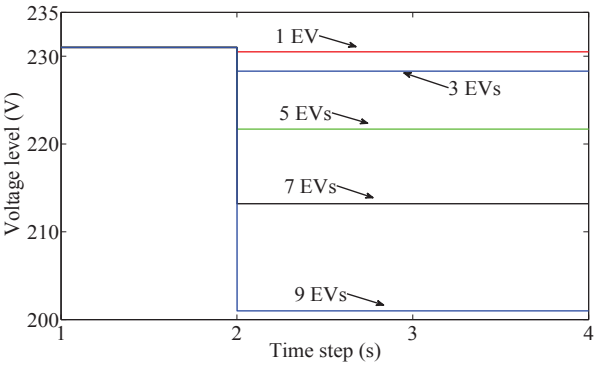

Fig. 7. Voltage dynamics at the furthest node from the transformer when multiple EVs begin to charge simultaneously.

dynamics, compared to the charging of the EVs. The reason for this is as follows. The productions of the PVs on the LV string are highly correlated leading to simultaneous variations in their productions, which leads to higher voltage and load dynamics. On the other hand, the probability that the EVs start charging exactly at the same time is very low as discussed above, thereby leading to slower voltage and load dynamics.

V. Communication Latency

In this section, we attempt to translate the voltage and load dynamics obtained from the simulations into telecommunication time requirements. First we assume that a control signal is initiated when the voltage or load level reaches 80% of the maximum bound (we will later present an analysis for other cases as well). From the results in Fig. 5 and Fig. 6, we have observed that the voltage level can rise from 80% overvoltage to the maximum bound in 600 ms, while the cable load can rise from 80% to 100% of the maximum capacity 500 ms, in the worst case. In practice, cable load control is less critical than voltage control because while cable overload can be tolerated for a short period of time, the voltage level should always be in the bounds. Thus, in the worst case, the voltage and load control should respond in 600 ms. Next, we will present how we map the response time, 600 ms, into the telecommunication time requirements.

The voltage and load control could be designed using either a centralized or distributed architecture. Whereas the communication in a distributed control architecture could be complex and depend on the control algorithm used, communication in a centralized control architecture is relatively simple. For our analysis, we choose a centralized control architecture, where each house has an agent that communicates with a central server across a telecommunication network. Each agent has two main functions: (1) it measures the voltage and load patterns in its proximity and communicates them to the central server, and (2) it controls its local devices to a set point provided by the central server. On the other hand, the central server makes decisions based on the data communicated by the agents, about the target control set points and communicates them to the agents. Thus, the control time latency of the centralized control architecture is the total amount of time it takes starting from measuring an event to controlling the devices to a new set point. The control cycle is composed of the following five components/segments. (1) *measurement time*: the time it takes to measure the event, e.g. fast rise in voltage level (2) *upward communication time*: the time it takes an agent to communicate the measured values to the central server (3) *computation time*: the time it takes the central server to analyze the measured values and choose control set points (4) *downward communication*: the time it takes the central server to communicate the control set points to the agents (5) *control time*: the time it takes the agent to control its local devices to a new set point, e.g. turning off a PV panel or turning a battery storage on. There is also additional response time of the voltage and load to settle to the desired voltage/load levels after setting the devices to the desired power production/consumption levels. But this response time can be considered negligible since the voltage and load levels adjust immediately with the change in the power flows.

TABLE I. Mapping control trigger point to latency constraint.

Trigger point (% overvoltage)	40	50	60	70	90	95
Latency constraint (s)	0.99	0.74	0.49	0.39	0.09	0.025

TABLE II. Typical latency overview of communication technologies (The latency values are adopted from [25]-[30])

	Example	Typical Latency
Fast dedicated infrastructure	optical fiber	$5\mu s$
Wired TCP/IP communication	DSL	40ms
Wireless communication	WiMax	10ms
Fast mobile communication	UMTS	150ms
Slow mobile communication	GPRS	500ms
Powerline communications	PLC	seconds

To measure power quality root mean square measurements are needed, which are calculated after measuring half a period. The frequency in the Dutch energy grid is 50 Hz, and therefore the measurement time is 10 ms. The computation time depends on the hardware used and the computation algorithm, which can be assumed to be in the order of milliseconds. The control time of batteries and PV panels is in the order of milliseconds. In this work, without loss of generality, computation time and control time are each assumed to be 5 ms. Deducting these times from the 600 ms response time, the upward and downward communication times are left with 600 ms - 20 ms = 580 ms. Thus, the communication technology should be able to handle one way communication in (580 ms)/2 =290 ms. In a similar fashion, the constraints on communication latency could be derived for the cases when other voltage levels initiate control. Table I presents the mapping from the voltage level where control is initiated to the communication latency constraint. The table reveals that if a control signal is triggered at an early stage of the voltage rise (further from the maximum bound), then we have a looser communication latency constraint that could be guaranteed by many of the telecommunication technologies. However, if the control signal is initiated after the voltage level is already close to the maximum bound, then we have a tight communication latency constraint that could be guaranteed by only a few of the telecommunication technologies. Table II provides approximate values of the typical latency of various groups of communication technologies. Apparently, installing

the technologies with smaller latency, such as the optical fiber, is more expensive.

Initiating the control signal too early before the maximum bound means that frequent control computations will take place at the server, even in the situations that might not pose a threat. Therefore, a designer needs to make a compromise between the cost of the telecommunication technologies and the frequency of control computation.

VI. Conclusions

In this paper, we provided a study regarding the last mile communication time requirements of the smart grid. We considered a low voltage power grid supporting a futuristic neighborhood with large penetration of distributed energy resources and electric vehicles, that could potentially lead to highly volatile voltage and load dynamics in the LV grid. To identify the telecommunication time requirements of the future smart grid, we selected the most time sensitive functions of the smart grid. Our findings indicate that voltage control poses the most critical communication time requirement compared to the other smart grid functions. Hence, the stringent communication time requirement of voltage control needs to be taken into account when choosing an appropriate telecommunication technology to support the future low voltage smart grids. The communication latency requirement could be as small as a few hundred milliseconds.

VII. Acknowledgment

This research has been supported by the EU FP7 Network of Excellence in Internet Science EINS (Project No. 288021).

References

[1] G. A. Pagani and M. Aiello, "Towards Decentralization: a Topological Investigation of the Medium and Low Voltage Grids," *IEEE trans. Smart Grids, vol. 2, n. 3, pp. 538-547, 2011.*

[2] E. Negeri, N. Baken, and M. Popov, "Holonic Architecture of the Smart Grid," Smart Grid and Renewable Energy, vol. 4, pp. 202-212, 2013.

[3] N. D. Hatziargyriou, A.P. Sakis Meliopoulos, "Distributed Energy Sources: Technical Challenges," IEEE Power Engineering Society Winter Meeting, vol.2, pp. 1017-1022, 2002.

[4] J. A. Pecas Lopes, F. j. Soares, and P. M. R. Almeida, "Integration of Electric Vehicles in the Electric Power System," Proceedings of the IEEE, vol. 99, no. 1, pp. 168-183, 2011.

[5] E. Negeri, and N. Baken, "Smart Integration of Electric Vehicles in an Energy Community," *In Proc. of the 1st Int. Conf. on Smart Grids and Green IT Systems, pp. 25-32, Apr. 2012.*

[6] Y. Yan, Y. Qian, H. Sharif, and D. Tipper, "A Survey on Smart Grid Communication Infrastructures: Motivations, Requirements and Challenges," *IEEE Communications Survey & Tutorials, 2012.*

[7] W. Luan, D. Sharp, and S. Lancashire, "Smart Grid Communication Network Capacity Planning for Power Utilities,âĂİ 2010 IEEE PES Transmission and Distribution Conference and Exposition, pp.1-4, 2010.

[8] D. Niyato and P. Wang, "Reliability Analysis and Redundancy Design of Smart Grid Wireless Communications System for Demand Side Management," Wireless Communications, IEEE, vol. 19, no. 3, pp. 38-46, 2012.

[9] J. Zhou, R.Q. Hu, and Y. Qian, "Scalable Distributed Communication Architectures to Support Advanced Metering Infrastructure in Smart Grid," IEEE Transactions on Parallel and Distributed Systems, vol. 23, no. 9, 2012.

[10] R. Yu, Y. Zhang, S. Gjessing, C. Yuen, S. Xie, and M. Guizani, "Cognitive Radio Based Hierarchical Communications Infrastructure for Smart Grid," IEEE Network, vol. 25, no. 5, pp. 6-14, 2011.

[11] Z. Fan, P. Kulkarni, S. Gormus, C. Efthymiou, G. Kalogridis, M. Sooriyabandara, Z. Zhu, S. Lambotharan, and W. H. Chin, "Smart Grid Communications: Overview of Research Challenges, Solutions, and Standardization Activities," *Communications Surveys and Tutorials, IEEE, 2011.*

[12] A. Aggarwal, S. Kunta, P. Verma, "A Proposed Communications Infrastructure for the Smart Grid," IEEE Innovative Smart Grid Technologies (ISGT), 2010.

[13] H. Georg, N. Dorsch, M. Putzke, and C. Wietfeld, "Performance Evaluation of Time-Critical Communication Networks for Smart Grids based on IEC 61850," IEEE INFOCOM Workshop on communications and Control for Smart Energy Systems, 2013.

[14] E. Negeri, and N. Baken, "Distributed Storage Management Using Dynamic Pricing in a Self-Organized Energy Community," *In Proceedings of 6th International Workshop on Self Organized Systems, pp. 1-12, 2012.*

[15] M.A. Kashem, V. Ganapathy, G.B. Jasmon, "A Geometric Approach for Three-Phase Load Balancing in Distribution Networks," International Conference on Power System Technology, Proceedings of PowerCon 2000, vol. 1, pp. 293-298.

[16] N. Leemput, F. Geth, B. Claessens, J. Van Roy, R. Ponnette, and J. Driesen, "A Case Study of Coordinated Electric Vehicle Charging for Peak Shaving on a Low Voltage Grid," IEEE Innovative Smart Grid Technologies (ISGT Europe), 2012.

[17] K. De Brabandere, B. Bolsens, J. Van den Keybus, A. Woyte, J. Driesen, R. Belmans, "A Voltage and Frequency Droop Control Method for Parallel Inverters," IEEE Transactions on Power Electronics, vol. 22, no. 4, pp. 1107-1115, 2007.

[18] K. D. Brabandere, "Voltage and Frequency Droop Control in Low Voltage Grids by Distributed Generators with Inverter Front-end," PhD Thesis, Katholieke Universiteit Leuven, ISBN 90-5682-745-6, 2006.

[19] J.K. Kok, B. Roossien, P.A. MacDougall, O.P. Pruissen, G. Venekamp, I.G. Kamphuis, J.A.W Laarakkers, and C.J. Warmer, âĂIJDynamic Pricing by Scalable Energy Management Systems - Field Experiences and Simulation Results using PowerMatcher,âĂİ IEEE Power and Energy Society General Meeting 2012, IEEE, 2012.

[20] A. Mohsenian-Rad, Vincent W.S. Wong, J. Jatskevich, R. Schober, and A. Leon-Garcia, "Autonomous Demand-Side Management Based on Game-Theoretic Energy Consumption Scheduling for the Future Smart Grid", *IEEE Transactions on Smart Grid, vol. 1, no. 3, pp. 320-331, 2010.*

[21] H. Yoshida, K. Kawata, Y. Fukuyama, S. Takayama, and Y. Nakanishi, "A Particle Swarm Optimization for Reactive Power and Voltage Control Considering Voltage Security Assessment," IEEE Transactions on Power Systems, vol. 15, no. 4, pp. 1232-1239, 2000.

[22] K.S. Verma, S.N. Singh, and H.O. Gupta, "Location of Unified Power Flow Controller for Congestion Management," Electric Power Systems Research, vol. 58, no. 2, pp. 89-96, 2001.

[23] Gaia LV Network Design [online]. Available: http://www.phasetophase.nl/en_products/vision_lv_network_design.html

[24] National Renewable Energy Laboratory (NREL), "Solar Measurement Grid (1-Year Archive)," availabble: www.nrel.gov/midc/oahu_archive/

[25] V. K. Sood, D. Fischer, J. M. Eklund, T. Brown, "Developing a Communication Infrastructure for the Smart Grid," Electrical Power and Energy Conference (EPEC), 2009.

[26] Verizon Communications, "IP Latency Statistics," [Online]. Available: http://www.verizonbusiness.com/about/network/latency/.

[27] Wimax.com, "Quality Of Service WiMAX," [Online]. Available: http://www.wimax.com/wimax-tutorial/quality-of-service.

[28] B. A. Akyol, H. Kirkham, S. L. Clements, M. D. Hadley, "A Survey of Wireless Communications for the Electric Power System," technical report, Pacific Northwest National Laboratory, 2010.

[29] Radio-electronics.com, "UMTS / WCDMA Basics Tutorial and Overview," [Online]. Available: http://www.radio-electronics.com/info/cellulartelecomms/umts/umts_wcdma_tutorial.php.

[30] F. Aalamifar, "Viability of Powerline Communications for the Smart Grid," 26th Biennial Symposium on Communications (QBSC), 2012.